doi:10.2533/chimia.2021.1004 Chimia 75 (2021) 1004–1011 © S. Matile *et al.*

Flipper Probes for the Community

Lea Assies[ab], José García-Calvo[ab], Francesca Piazzolla[abj], Samantha Sanchez[abj], Takehiro Kato[ab], Luc Reymond[ac], Antoine Goujon[abj], Adai Colom[adj], Javier López-Andarias[ab], Karolína Straková[abj], Dora Mahecic[ae], Vincent Mercier[ad], Margot Riggi[adfj], Noemi Jiménez-Rojo[ad], Chloé Roffay [ad], Giuseppe Licari[gj], Maria Tsemperouli[ahj], Frederik Neuhaus[ahj], Alexandre Fürstenberg[gi], Eric Vauthey[g], Sascha Hoogendoorn[ab], Marcos Gonzalez-Gaitan[ad], Andreas Zumbuehl[ahj], Kaori Sugihara[agj], Jean Gruenberg[ad], Howard Riezman[ad], Robbie Loewith[af], Suliana Manley[ae], Aurelien Roux[ad], Nicolas Winssinger[ab], Naomi Sakai[ab], Stefan Pitsch[c], and Stefan Matile*[ab]

Abstract: This article describes four fluorescent membrane tension probes that have been designed, synthesized, evaluated, commercialized and applied to current biology challenges in the context of the NCCR Chemical Biology. Their names are Flipper-TR®, ER Flipper-TR®, Lyso Flipper-TR®, and Mito Flipper-TR®. They are available from Spirochrome.

Keywords: Flipper probes · Fluorescence imaging · NCCR Chemical Biology

The development of new chemistry tools has enabled some of the most essential discoveries in biology. While the research challenges involved are understood and cherished, the importance of availability and guiding examples for use are easily underestimated or even ignored in academia. One of the goals of the National Centre of Competence in Research (NCCR) Chemical Biology was to provide network and infrastructure that would allow to realize this process from the beginning to the end. The fluorescence imaging of membrane tension or physical forces in general in living cells was identified as an important need in biology. The proof of concept was published almost ten years ago.[1] The operational flipper probes appeared in 2015,[2] compatibility with cells in 2016[3] and the quantitative calibration of fluorescence lifetime against the physical force in 2018.[4] Published on the same day, the first example of how to use flipper probes to elucidate how membrane tension governs signal transduction appeared.[5] Within one week after publication, more than 50 requests for probes from research groups all over the world were received. In response to this demand, the University of Geneva agreed to license the distribution of flipper probes to Spirochrome. The initial Flipper-TR® **1** became available at the end of 2018 (Fig. 1). Three more probes, namely ER Flipper-TR® **2**, Lyso Flipper-TR® **3**, and Mito Flipper-TR® **4**, followed in September 2020, after their introduction in 2019[6] and together with NCCR examples of how to use them to elucidate the mechanics of endocytosis[7] and mitochondrial fission.[8] Hundreds of samples have since been distributed all over the world. Many biology groups expressed their gratitude and joy to finally be able to do their long-dreamed-about experiments.

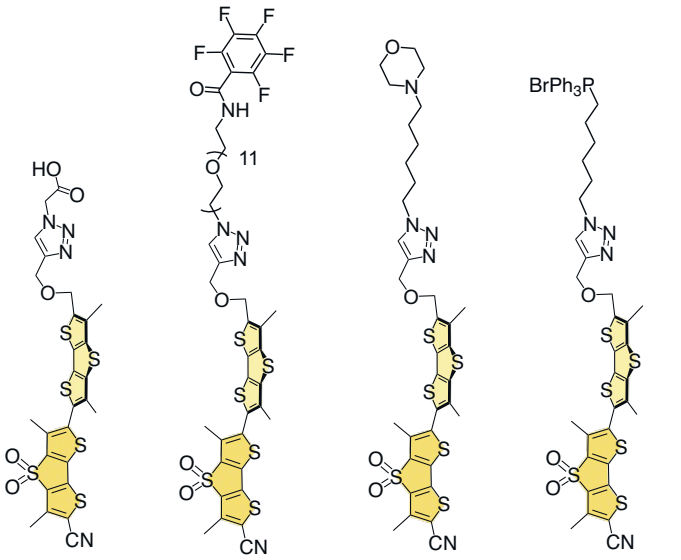

Fig. 1. Chemical structure of the four commercialized fluorescent membrane tension probes.

Production

The main challenge for commercialization is the scale-up of top-quality material. For flipper probes, this is a significant effort. Today, the original Flipper-TR® **1** is synthesized in 15 steps from tetrabromothiophene **5** (Scheme 1). This synthesis has been improved over the years, particularly during scale-up for commercialization, and has never been published in complete, updated form. The general challenge is the poor solubility of most synthetic intermediates. Oxidized dithienothiophenes (DTTs) are particularly intractable.

The first step is the reaction with two equivalents of acetaldehyde **6**, an unproblematic nucleophilic addition *via* lithiation with *n*-BuLi. After addition of **6** at –78 °C, the solution becomes very viscous and has to be warmed to room temperature to continue stirring for 1 hour. The resulting diol **7** is directly oxidized with sodium dichromate to yield the diketone **8** in 74% over two steps. A beautiful cascade cyclization with ethyl 2-mercaptoacetate **9** affords the DTT core in 90% yield. Diester **10** is hydrolyzed, and the

*Correspondence: Prof. S. Matile[ab], E-mail: stefan.matile@unige.ch
[a]National Centre of Competence in Research (NCCR) Chemical Biology, 30 Quai Ernest-Ansermet, CH-1211 Geneva, Switzerland;
[b]Department of Organic Chemistry, University of Geneva, 30 Quai Ernest-Ansermet, CH-1211 CH-Geneva, Switzerland;
[c]Spirochrome AG, Chalberwiesenstrasse 4, CH-8260 Stein am Rhein, Switzerland;
[d]Department of Biochemistry, University of Geneva;
[e]École Polytechnique Fédérale de Lausanne – EPFL, SB Cubotron 427, CH-1015 Lausanne, Switzerland;
[f]Department of Molecular Biology, University of Geneva;
[g]Department of Physical Chemistry, University of Geneva;,
[h]Department of Chemistry, University of Fribourg, 9 Chemin du Musée, CH-1700 Fribourg, Switzerland;
[i]Department of Inorganic and Analytical Chemistry, University of Geneva;
[j]Current addresses are not indicated

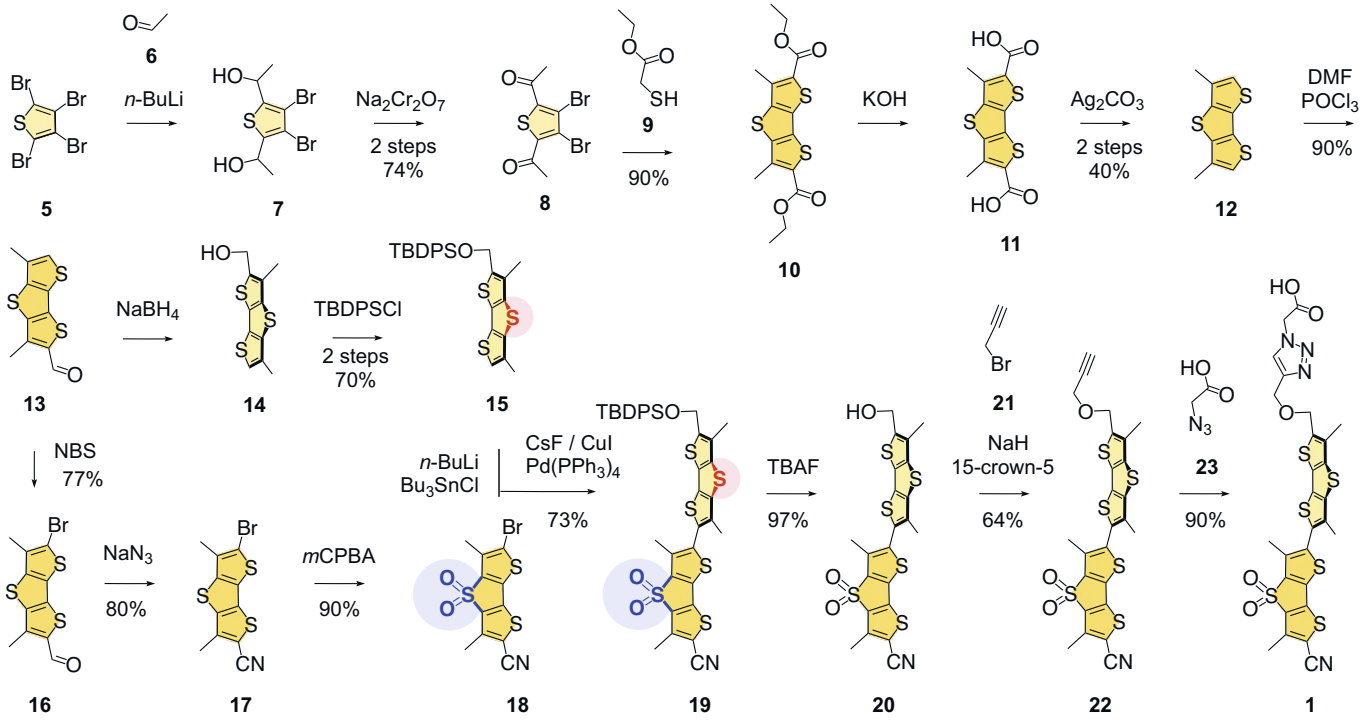

Scheme 1. The total synthesis of Flipper-TR® **1**.

resulting diacid **11** is decarboxylated to yield the α-unsubstituted DTT **12**.[9] To reach 40% yield, it is particularly important to thoroughly dry the diacid **11** before the reaction.

A very clean Vilsmayer-Haack monoformylation leads to aldehyde **13**. Here, the synthetic route splits in two directions to prepare the two DTT monomers needed for their Stille coupling into the twisted dimer. On the one side, the aldehyde is reduced, and the resulting alcohol **14** is protected as silyl ether **15**. The use of bulky TBDPS ethers is essential to improve solubility over the next two steps. On the other side, the first key intermediate **13** is brominated, and the formyl group of the resulting DTT **16** is transformed into the final cyano acceptor. The resulting pseudo-sulfide **17** is oxidized to the pseudo-sulfone **18**.[2,10] Careful monitoring of reaction conditions with 3 equiv. *m*CPBA added over 5 h allows to reach 90% yield.

The Stille coupling of donor **15** and acceptor **18** has been challenging for scale-up because of fluctuating yields. The addition of CsF and CuI provided much improvement,[11] the use of LDA instead of *n*-BuLi and limitation of the reaction time to 16 h as well. Under these conditions the flipper scaffold **19** can be obtained in 64% to maximal 73%. With the routine removal of the TBDPS protecting group with TBAF, solubility becomes very low, complicating also purification. Williamson ether synthesis with alcohol **20** and alkyne **21** can be improved from the reported 20% with the addition of 0.1 equiv. 15-crown-5 to NaH before addition of propargylbromide **21**. After 3 h, the alkyne **22** can be isolated in 55% to maximal 64% yield. The final click reaction occurs in 90% yield, although purification of the Flipper-TR® **1** is as challenging as the combination of fatty acid like amphiphilicity with intrinsically poor solubility implies.[2,3,10]

Contrary to intermediates **19**–**22**, the chemical stability of Flipper-TR® **1** is satisfactory because the triazole is not only there for synthetic convenience but also to prevent transient protonation of the thenyl ether, which triggers headgroup elimination by acid-catalyzed activation of the leaving group. The purity of Flipper-TR® **1** is verified by ^{1}H and ^{13}C NMR spectroscopy (Fig. 2), and by HPLC. Precise aliquot concentrations are determined from the absorption maximum in organic solvent, and all new compounds are tested for correct performance in cells.

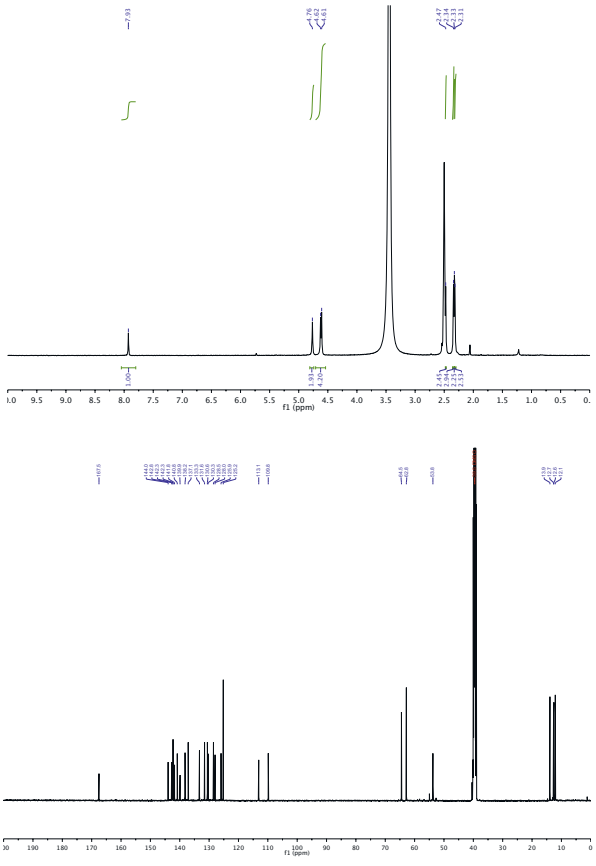

Fig. 2. Representative original ^{1}H and ^{13}C NMR spectra of Flipper-TR® **1** in DMSO-d_6/D_2O with ND_4OD.

The synthesis of flippers **2**–**4** with modified headgroups conveniently diverges from Flipper-TR® **1** on the last click with flipper **22** (Scheme 2).[6] Different to reported procedures, ER Flipper-TR® **2** is best prepared by coupling first the amine **23** with the acyl chloride **24**. The following click reaction with azide **25** and flipper **22** yields the target molecule in 71%, which is easier to purify because it is not amphiphilic.

The similarly straightforward synthesis of Lyso Flipper-TR® **3** requires first bromide **26** to alkylate morpholine **27**. The resulting alcohol **28** is then transformed into azide **29**, which is clicked on flipper **22** to afford target molecule **3**. For Mito Flipper-TR® **4**, alkyl bromide **26** is reacted first with triphenylphosphine. The resulting phosphonium salt **30** is then transformed as before into the azide **31** and clicked with **22** to afford target flipper **4**.

Taken together, flipper synthesis is challenging but feasible also in larger quantities. Flipper probes in general are a great example that fundamental supramolecular chemistry concepts (*vide infra*) and demanding multistep synthesis do not exclude practical usefulness as long as the addressed challenge is sufficiently important.

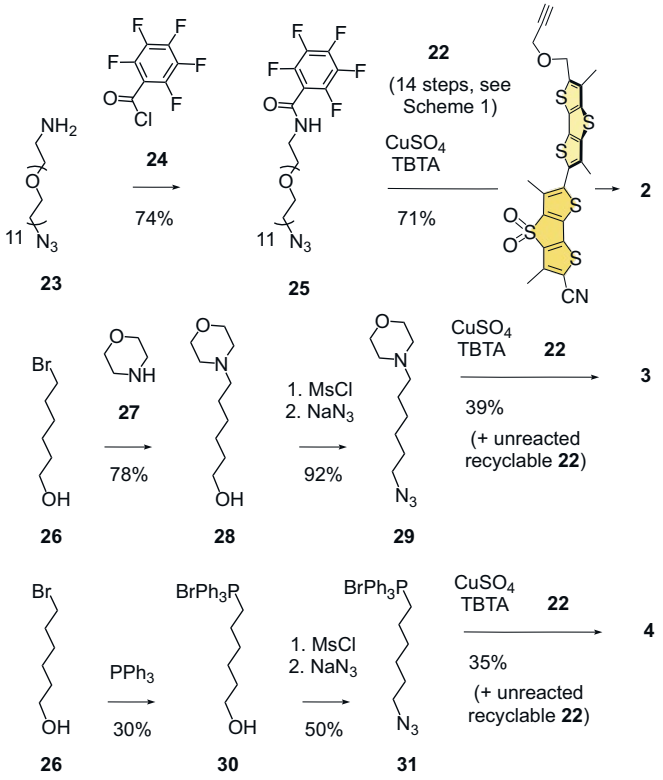

Scheme 2. The total synthesis of ER Flipper-TR® **2**, Lyso Flipper-TR® **3** and Mito Flipper-TR® **4**.

Common Characteristics

While the four commercialized flipper probes target different membranes in cells (*vide infra*), their bioinspired[12–14] mechanochemistry is identical. In their ground state, the two DTT chromophores are twisted out of co-planarity (Fig. 3). This twist originates from 'chalcogen-bonding'[15–20] repulsion between the methyls and the σ holes on the sulfurs next to the twistable bond that connects the two DTTs. The electrostatic origin of the twist is important, because steric twisting would exclude planarization. This twisted dimer is equipped with donors D at one and acceptors A at the other end. The pseudo-sulfide and pseudo-sulfone bridges in the two DTTs act as endocyclic D_n and A_n, respectively. They are supported by a cyano group as exocyclic A_x and a thienyl ether as non-covalent but essential D_x. On the donor side, the two other sulfurs plus the methyl groups can further contribute as conjugated donors, as indicated with bold bonds in the planarized flipper mesomer.

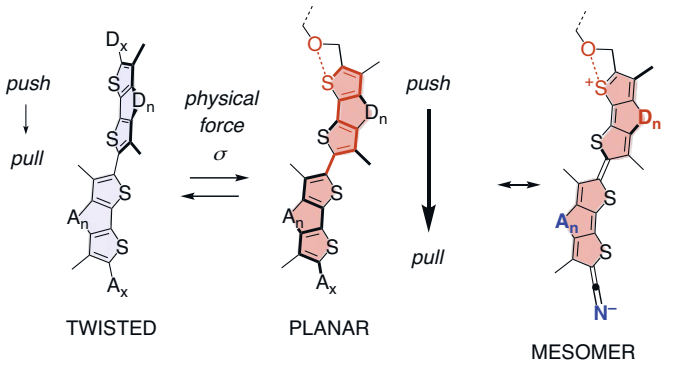

Fig. 3. Flipper design as planarizable push-pull probe with generalized endo- and exocyclic donors and acceptors. One of many mesomers is shown to illustrate the emergence of the push-pull system by mechanical planarization.

Mechanical planarization of the twisted flipper increases the conjugation and thus connects the donors and acceptors. One of many possible mesomers is drawn to highlight the resulting push–pull chromophore, with a rigid formal double bond connecting the two DTTs and electrons flowing from donor to acceptor, resulting in a formal positive charge on the former and a formal negative charge on the latter. For the non-covalent D_x, the formal positive charge on the sulfur deepens the σ holes to form a strong chalcogen bond that injects electron density from the ether oxygen.

In organic solvents, the absorption and excitation maxima are blue shifted near 400 nm. In liquid-disordered (L_d) lipid bilayer membranes, the excitation slightly red shifts to a broad maximum around 430 nm (Fig. 4, blue).[21,22] In liquid-ordered (L_o) and in solid-ordered (S_o) membranes, the excitation significantly red shifts to an overall maximum at 490 nm (Fig. 4, red). The appearance of vibrational fine structure allows to further deconvolute the spectra, which affords a 0–0 transition at 515 nm.[21] The red shift with increasing membrane order coincides with a strong increase in fluorescence intensity and fluorescence lifetime. This also increases the fluorescence quantum yield, which is at 25% in ethyl acetate[3] but less quantifiable in membranes. Shifts of the emission maximum around 600 nm are less significant and less reliable (possibly related to hydration, considering strong solvatochromism in emission).

These spectroscopic properties are consistent with the following energy diagram (Fig. 4). Excitation of a relaxed, twisted ground state (GS) produces a high energy Franck-Condon (FC) excited state (ES) of identical twist (Fig. 4, blue pathways). According to time-resolved emission, mechanosensitive ES planarization supported by intramolecular charge transfer occurs within ~4 ps.[10] Emission from the resulting planar intramolecular charge transfer (PICT) ES produces a planar GS that relaxes into the twisted GS minimum. ES planarization from the twisted FC state competes with ES deplanarization for nonradiative decay through various pathways including conical intersections, possibly TICT.

Upon mechanical planarization in the GS, flipper excitation into a similarly planarized ES accounts for the observed red shift in excitation (Fig. 4, red pathway). ES planarization to the PICT ES is independent of GS twisting, which explains the poor mechanosensitivity of the emission maximum. ES deplanarization from a less twisted FC ES is less favorable, which explains increases in fluorescence intensity and lifetime upon planarization.

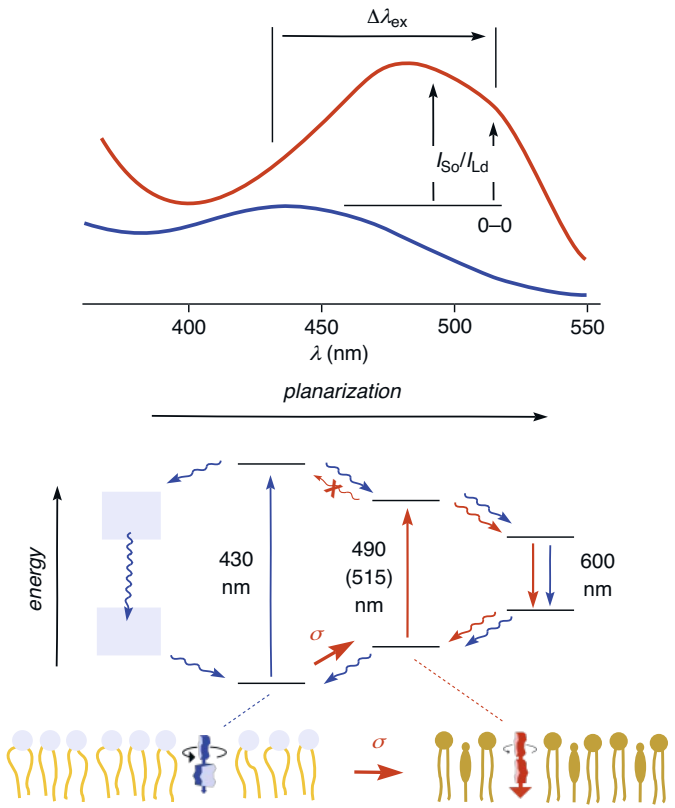

Fig. 4. Schematic excitation spectra and energy diagram of more twisted flippers in L_d (blue) and more planar flippers in L_o/S_o membranes (red). σ = mechanical force to planarize flippers in the ground state.

Fluorescence lifetime imaging microscopy (FLIM) is attractive for live cell experiments because lifetimes are concentration independent, and effective concentrations are difficult to know and control in cells. FLIM images of flippers **1**–**4** in GUVs confirmed lifetimes measured spectroscopically in LUVs (Fig. 5).[6] In L_d membranes, the $\tau = 3.8$–2.9 ns corresponded with blue shifted excitation of twisted flippers. In S_o membranes, the $\tau = 6.4$–5.5 ns corresponded with red shifted excitation of planarized flippers. Note the anisotropy in the images of L_o but not L_d GUVs under linearly polarized excitation, confirming more uniform flipper orientation parallel to lipid tails in the latter.[23]

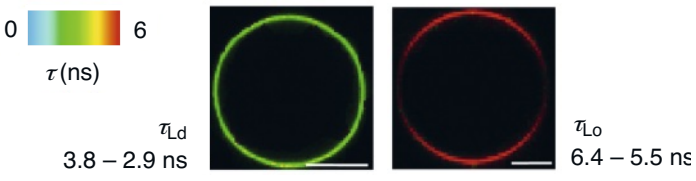

Fig. 5. FLIM image of more twisted flippers in L_d (green) and more planar flippers in L_o/S_o GUVs (red), with the lifetime range covered by **1**-**4**. Scale bar: 10 μm. Adapted from ref. [6], copyright American Chemical Society 2019.

The response of flipper probes to membrane tension applied to GUVs by micropipettes or osmotic stress has been monitored by FLIM.[4] The measured lifetimes have been quantitatively calibrated to the applied forces from the diameter of nanotubes pulled from GUVs with optical tweezers. In homogenous membranes, increasing tension resulted in decreasing lifetimes, which is consistent with flipper deplanarization upon lipid decompression (Fig. 6b). The slope of the roughly linear response up to $\sigma > 0.5$ mN/m depended on the nature of the lipids. In mixed membranes, increasing tension resulted in increasing lifetimes, consistent with membrane reorganization and planarized flipper in non-stretchable highly ordered microdomains dominating the response (Fig. 6a). Tension-induced phase separation was demonstrated in GUVs. Particularly upon decreasing tension (or increasing compression), contributions beyond microdomain dis/assembly such as changes in membrane curvature, from rippling, buckling and budding to tubules extending from the membrane and excess lipid being ejected, become increasingly important.[24] These changing contributions do not change the final response in mixed membranes, that is decreasing lifetimes (flipper deplanarization) with decreasing tension (or increasing compression).

Membrane tension applied to cells consistently increased flipper lifetimes, independent on flipper location, indicating that the response is dominated by membrane reorganization, mostly tension-induced microdomain assembly (Fig. 6a).[4] Membrane tension applied to cells by hyperosmotic stress caused the corresponding shortened flipper lifetimes, indicative for dominant response from microdomain disassembly and membrane deformation. The changes in membrane tension are not always directly visible in FLIM images (Fig. 7a).[25] However, analysis of histograms from FLIM images reveals clear changes in lifetime (Fig. 7b).[6] Statistical analysis of the lifetime changes with membrane tension in different experiments then affords average lifetime changes with accuracies exceeding 0.1 ns (Fig. 7c).[25]

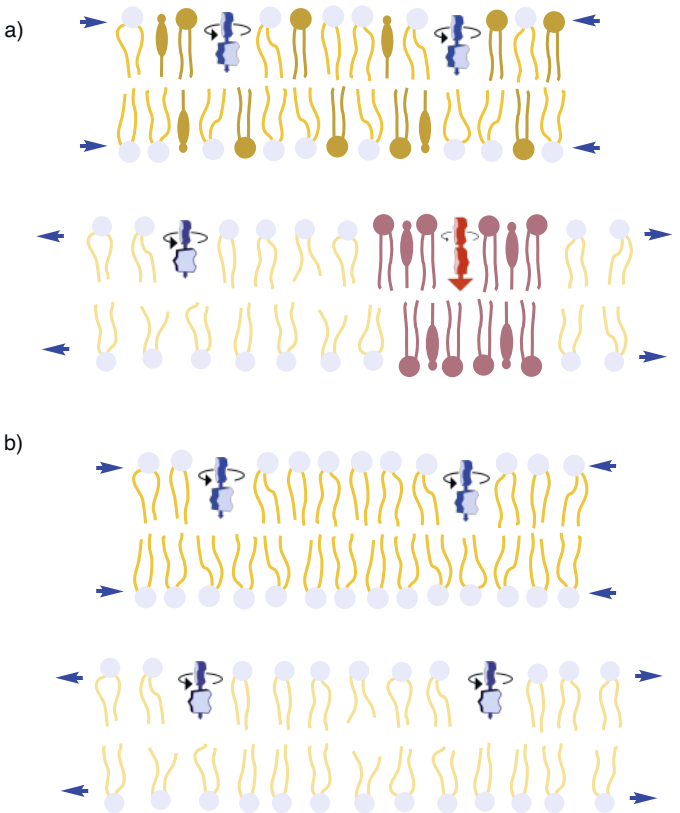

Fig. 6. a) In mixed membranes, increasing flipper lifetimes with increasing tension report on membrane reorganization, with dominant response from microdomain out-sorting, and decreasing lifetimes with decreasing tension on microdomain disassembly. b) In uniform membranes, decreasing lifetimes with increasing tension report on lipid decompression.

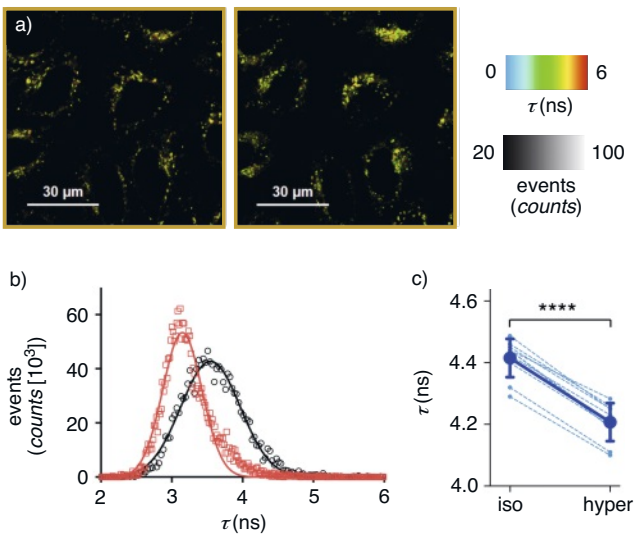

Fig. 7. a) Representative FLIM images of HeLa cells with Lyso Flipper-TR® **3** before (left) and after (right) hyperosmotic shock. b) Representative FLIM histogram of COS7 cells with ER Flipper-TR® **2** before (black) and after (red) hyperosmotic shock, counting only sheets. c) Representative analysis of FLIM histogram of HeLa cells with Lyso Flipper-TR® **3** before and after hyperosmotic shock. Each line connects values from individual experiments, with error bars depicting the mean ± SD, ****P < 0.0001, Student's t-test. a, c) Adapted from ref. [23], Supporting Information, copyright Wiley 2021. b) Adapted from ref. [6], copyright American Chemical Society 2019.

All four flipper probes can be directly added to unmodified cells. Removal of excess probe by washing is not required because probe fluorescence outside of membranes is negligible. Without applied tension, average lifetimes in FLIM images report on the average order in the membrane of interest (MOI). High order corresponds to long lifetimes. At constant lipid composition in the MOI, applied membrane tension is reported from tension-induced membrane reorganization. For the reasons discussed above, increasing tension corresponds to increasing lifetimes.

Flipper-TR®

The original Flipper-TR® **1** selectively labels the plasma membrane (PM, Fig. 8e). The selectivity originates from the carboxylate anion in the headgroup, which prefers to stay at the membrane surface. Unpublished results demonstrate that the outer leaflet of the plasma membrane is labeled selectively (Fig. 8a). Flip flop is slow on the experimental timescale. Moreover, partitioning is reversible and transfer between outer leaflets of different membranes is fast. Strategies to selectively label the inner leaflet of plasma membranes with Flipper-TR® **1** exist and will be published soon.

The fluorescence lifetime of Flipper-TR® **1** in plasma membranes varies with their composition in different cells. Different lifetimes in MOIs at rest do not reflect only differences in membrane tension but mostly differences in membrane composition and organization. Consistent with the highly ordered plasma membrane phases, fluorescent flipper lifetimes are generally very long. In HeLa cells, for instance, τ_{av} = 4.8 ns has been measured (Fig. 8a,e).[6] Consistent with microdomain disassembly and membrane deformations, the application of hyperosmotic stress reduced this lifetime to 4.2 ns. By now, Flipper-TR® **1** has been measured in the plasma membrane of many different cells (*vide infra*).

An example of the use of Flipper-TR® **1** to address topics of current concern in biology has been provided with studies aimed at defining the role of TORC2 (target of rapamycin complex 2) in regulation of PM dynamics.[5,26] It was demonstrated that increase or decrease in PM tension, triggered through orthogonal means, respectively increases or decreases the kinase activity of TORC2. *Vice versa*, chemical-genetic approaches that activate or inhibit TORC2 kinase activity, respectively decrease or increase PM tension. Thus, Flipper-TR® **1** experiments enabled the authors to conclude that TORC2 functions in a negative feedback loop to maintain PM tension within a narrow window optimized for its many structural and biochemical functions.[27] Such a function for TORC2 in mechanotransduction was unexpected as TOR is better appreciated for its role in nutrient signaling. If loss of PM tension homeostasis plays a role in diseases associated with mammalian TOR dysfunction will be important to consider in the future.

In model membranes consisting of POPC and either phosphatidylcholine or ceramide, Flipper-TR® **1** has been of use to demonstrate the effect of the physico-chemical properties and behavior of sphingolipids and ether lipids in membranes along the secretory pathway.[28] Flipper-TR® **1** in HeLa cells has been of use to relate the changes in cell volume and membrane tension during osmotic shocks.[29] Tension and volume recovered from hypoosmotic shocks but not from hyperosmotic shocks.

ER Flipper-TR®

The ER Flipper-TR® **2** selectively labels the membranes of the endoplasmic reticulum (Fig. 8f).[6] The selectivity originates from the pentafluorophenyl group, which is thought to react with cysteines in proteins at the outer surface of the ER (Fig. 8b). Because the distance of these cysteines from the membrane is unknown and can be significant, a long PEG tether is inserted between the pentafluorophenyl tracker and the flipper in **2**. Co-localization in CLSM images with commercially available ER trackers is nearly perfect (Pearson correlation coefficient PCC = 0.9).

The average fluorescence lifetime of ER Flipper-TR® **2** in the ER of COS7 cells was 3.5 ns. This compared to PM short lifetime cannot be correlated to differences in membrane tension. In general, lifetimes of MOIs in resting conditions may reflect either different tensions, or different lipid order, or combinations of both. This includes contributions from lipid composition and different domains, maybe also proteins. The short average lifetime of the ER membranes compared to the plasma membranes is consistent with the overall lower order of these membranes. The large ER provided the perfect example to illustrate that lifetimes do not have to be homogenous for an organelle. In COS7 cells, flippers in a thin meshwork attributed to tubular ER showed a fluorescence lifetime of 4.1 ns. ER sheets around the nucleus were with 3.5 ns clearly less ordered. A similar lifetime of 3.4 ns for the nuclear envelope was reasonable considering that the two are connected and that tension gradients exist.

Hyperosmotic stress lowered the average lifetime of ER Flipper-TR® **2** in COS7 cells from 3.5 to 3.3 ns. In HeLa cells, a decrease from 3.4 to 3.0 ns was observed. Isolated changes in ER sheets were in the same range (Fig. 7b). These changes were consistent with operational mechanosensitivity of ER Flipper-TR® **2**, reporting membrane tension changes in the ER with changes in fluorescence lifetime.

In contrast to immobile ER Flipper-TR® **2**, SupraFlippers can be released in the ER and stain the membranes along the secretory pathway.[30]

Lyso Flipper-TR®

The Lyso Flipper-TR® **3** selectively labels the membranes of lysosomes and late endosomes but not early endosomes (Fig. 7a).[6] The selectivity originates from unidirectional penetration along a pH gradient (Fig. 8c). The pH within late endosomes and lysosomes is <5.7. The pK_a of the morpholinium cation is 7.4. In neutral water, Lyso Flipper-TR® **3** is thus partially deprotonated and can diffuse in neutral form across endo-lysosomal membranes. Inside endo-lysosomes at pH <5.7, Lyso Flipper-TR® **3** is completely and permanently protonated and cannot move back into the cytosol.

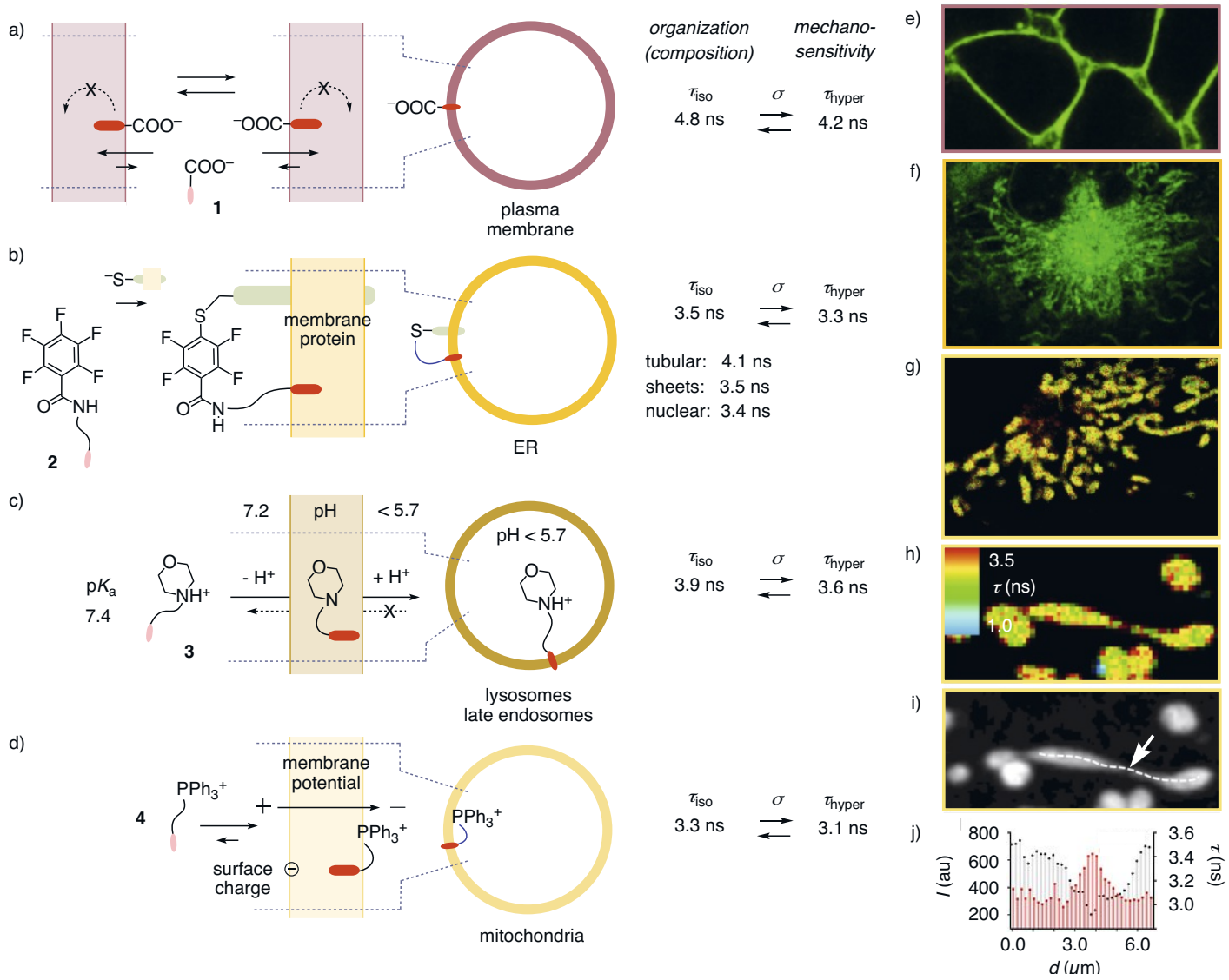

Fig. 8. Targeting mechanism, fluorescence lifetime without (iso) and with osmotic stress (hyper) informing on membrane order and tension, respectively for a) Flipper-TR® **1**, b) ER Flipper-TR® **2**, c) Lyso Flipper-TR® **3** and d) Mito Flipper-TR® **4**. e-j) Selected images for e) **1** in plasma membranes (HeLa, CLSM), f) **2** in ER (COS7, CLSM), g) **4** in mitochondria (COS7, FLIM), with h, j) lifetime and i, j) intensity along mitochondrial constriction. e-j) Adapted from ref. [6], copyright American Chemical Society 2019.

The flippers thus accumulate in the acidic organelles. The pH = 6.3 of early endosomes is insufficient to retain the probe.[25]

According to co-localization with commercial Lyso Trackers in CLSM images with a PCC = 0.9, the labeling of lysosomes and late endosomes with Lyso Flipper-TR® **3** is nearly perfect.[6] The average fluorescence lifetime of Lyso Flipper-TR® **3** in FLIM images of COS7 cells was 3.9 ns. This relatively high membrane order was in agreement with the origin of lysosomes and late endosomes from the plasma membrane. Hyperosmotic stress lowered the average lifetime of Lyso Flipper-TR® **3** in COS7 cells from 3.9 to 3.6 ns. In HeLa cells, lifetimes decreased similarly from 3.7 to 3.3 ns. These lifetime changes in response to membrane tension were in the range found with other flippers and thus consistent with operational mechanosensitivity of Lyso Flipper-TR® **3**.

As an example for the use of Lyso Flipper-TR® **3** to address biology topics of current concern, the membrane tension of organelles has been demonstrated to regulate the formation of intralumenal-vesicles (ILV), the endosome trafficking and their functions (notably intracellular traffic).[7]

Mito Flipper-TR®

The Mito Flipper-TR® **4** selectively labels the membranes of mitochondria (Fig. 8g).[6] The selectivity originates from the attraction of the hydrophobic triphenylphosphonium cation to the negatively charged surface and the inside negative potential of the mitochondrial membranes (Fig. 8d). In CLSM images, commercial Mito Trackers and **4** co-localize with a PCC = 0.9. The average fluorescence lifetime of Mito Flipper-TR® **4** in FLIM images of COS7 cells was 3.3 ns. This relatively low membrane order was in agreement with expectations. Hyperosmotic stress shortened the average lifetime to 3.1 ns. Identical changes at similar values from 3.2 to 3.0 ns were found in HeLa cells. These lifetime changes in response to membrane tension were in the usual range and thus confirmed the Mito Flipper-TR® **4** operates as membrane tension probe for mitochondria.

The use of Mito Flipper-TR® **4** to address biology topics of current concern has been illustrated early on with the increase of membrane tension in mitochondrial constrictions on the way to mitochondrial fission (Fig. 8h–j).[6,8] These constriction sites can eventually divide or reverse upon disassembly of the machinery. The use of Mito Flipper-TR® **4** revealed that tension at the constriction site is predictive of the outcome, more tensed constrictions having higher probability of fission.[8] Along these lines, Mito Flipper-TR® **4** helped to elucidate key molecular and cellular factors in the outer mitochondrial membrane during mitochondrial fission.

Reception

As mentioned in the introduction, hundreds of samples have been distributed since the commercialization of **1** in late 2018 and **2**–**4** in 2020. Flipper-TR® **1** has so far appeared in 16 publications, including the four from the NCCR community mentioned above.[5,26,28,29] The three other flippers, available only recently, have so far appeared in three NCCR publications (*vide supra*).[7,8,30]

Beyond the NCCR network, Flipper-TR® **1** has been used to analyze membrane tension in cells within a 3D matrix (and therefore inaccessible *via* optical trapping).[31] Live cells showed a striking decrease in fluorescence lifetime specifically at the cell rear, suggesting that in-plane membrane tension is significantly lower at the rear of cells. Zuttion *et al.* studied the lipopeptide daptomycin effect under infection-like conditions and compared with liquid-suspended vesicles and supported-membranes using electron and optical microscopies and Flipper-TR® **1**, where it was found that the cells with a healthier state of their cell wall show smaller membrane deformations.[32] Wang *et al*. studied the effect of enzymatically inserting synthetic lipids to increase cell membrane tension and inducing cell death, following the effects thanks to Flipper-TR® **1**.[33] Wong *et al.* engineered hydrogels to reveal how cells sense and respond to 3D biophysical cues.[34] Flipper-TR® **1** readily diffuses into alginate gels and labels the membrane of encapsulated mesenchymal stem cells (MSCs) following changes in these membranes after inserting hydrogels. Wang *et al.* used Flipper-TR® **1** as a fluorescent lipid tension sensor to determine membrane tension in mature adipocytes.[35] This is of interest because white adipose tissue (WAT) expansion in obesity occurs through enlargement of preexisting adipocytes (hypertrophy) and through formation of new adipocytes (adipogenesis). Sansen *et al.* investigated the mechanical, chemical and dynamic state of the cellular membranes using soft-gel nanoimprint lithography (soft-NIL) patterned nanostructures, where Flipper-TR® **1** is applied to measure the difference in membrane tension in HeLa cells depending on their position on the template.[36] Rahman *et al.* examine the inhibition of viral entry through interferon-inducible transmembrane protein 3 (IFITM3) and use Flipper-TR® **1** in HEK293T cells to visualize increased membrane order through IFITM3 oligomers.[37] Oberhauser *et al.* apply Flipper-TR® **1** in their study to assess changes in membrane tension in INS-1E β-cells before and after treatment with palmitate and oleate.[38] Nava *et al.* investigate how the genome is protected against mechanical stress and use in this context Flipper-TR® **1** to observe decreased fluorescence lifetime in perinuclear membranes after mechanical stretching, proving an increased nuclear deformability.[39] Gupta *et al* showed that Myoferlin overexpression in certain cancer cells expand its localization to the endo-lysosomal pathway, providing a modified tension measured with Flipper-TR® **1**, and higher membrane repair capacities.[40] To study the connection of plasma membrane cholesterol and glycolytic activity of the host cell during HIV-1 entry and fusion, Coomer *et al.* employ Flipper-TR® **1** to determine the effects of acute glycolysis inhibition in TZM-bI cells and compare to cholesterol depleted or supplemented cells.[41] Schneider *et al.* study how electrophilic thiol-reactive CPP additives efficiently create nucleation zones on the cell surface, which afterwards enable efficient transmission of the protein-CPP conjugates and use Flipper-TR® **1** to show a reduction of membrane tension at nucleation zones.[42]

Alternative Probes

Considering that flipper probes detect membrane order and tension-induced changes in membrane order, one would expect that many other membrane probes should qualify as tension probes. So far, such probes, if explored, have not yet delivered similarly consistent data sets. This difficulty to image membrane tension reliably could originate from the many, often demanding prerequisites an operational probe has to fulfill (spectroscopic properties, non-selective partitioning, positioning in membrane, compatibility with membrane organization, background fluorescence, delivery, intermembrane transfer, flip-flop, *etc.*).[2–4,43–45] Extensive failure with minor structural changes of flipper probes support that the correct balance of these parameters is subtle, challenging to find and easy to lose.[21,22] Moreover, flippers are the only probes that mechanically sense forces in equilibrium in the ground state. Other probes operate off-equilibrium in the excited state. The most developed Nile Red and Di-4-ANEPPDHQ solvatochromes report on membrane hydration in the excited state.[46,47] Direct comparison reveals that membrane hydration in response to membrane tension depends strongly on the nature of the MOI and is thus less suitable for reliable tension imaging, whereas flipper compression in the ground state as response to membrane tension is less MOI dependent.[48] Molecular rotors measure the kinetics of deplanarization in the excited state and report on viscosity (flippers do not[49]).[24,50,51] Same for papillons[52] and 'FLAPpers',[53] reporting on unbending in the excited state. ESIPT probes have proton transfer in the excited state in their name.[54] Only dynamers should report on mechanics in the ground state, but their fluorescence is so far insufficient.[55]

Future Flippers

Several new flipper probes have already been realized and wait for commercialization. EE Flippers target the early endosomes missed by the Lyso Flipper-TR® **3**.[25] HaloFlippers label the surrounding of HaloTags engineered into the MOI.[56] SupraFlippers integrate RUSH technology, target locally expressed streptavidin first and are then released with biotin.[30] PhotoFlippers release Flipper-TR® **1** in any MOI.[57] New blinking flipper architectures have been introduced to achieve compatibility with superresolution microscopy.[58] In HydroFlippers, the same architectures are used to simultaneously image changes in membrane compression and hydration, with the former being less dependent of the nature of the membrane and thus preferable to reliably image membrane tension.[48] This complementary behavior is important because it supports Flipper-TR® **1**, ER Flipper-TR® **2**, Lyso Flipper-TR® **3**, and Mito Flipper-TR® **4** as so far unique, robust and reliable small-molecule chemistry tools to routinely image membrane tension, without the need of genetic engineering, by simple addition to living cells, made available for the community as outlined in this article.

Acknowledgments

We warmly thank all former and present coworkers and collaborators who contributed to this research, and the University of Geneva, the NCCR Chemical Biology, the NCCR Molecular Systems Engineering, and the Swiss NSF for financial support.

Received: September 1, 2021

[1] A. Fin, A. Vargas Jentzsch, N. Sakai, S. Matile, *Angew. Chem. Int. Ed.* **2012**, *51*, 12736, https://doi.org/10.1002/anie.201206446.
[2] M. Dal Molin, Q. Verolet, A. Colom, R. Letrun, E. Derivery, M. Gonzalez-Gaitan, E. Vauthey, A. Roux, N. Sakai, S. Matile, *J. Am. Chem. Soc.* **2015**, *137*, 568, https://doi.org/10.1021/ja5107018.
[3] S. Soleimanpour, A. Colom, E. Derivery, M. Gonzalez-Gaitan, A. Roux, N. Sakai, S. Matile, *Chem. Commun.* **2016**, *52*, 14450, https://doi.org/10.1039/C6CC08771J.
[4] A. Colom, E. Derivery, S. Soleimanpour, C. Tomba, M. D. Molin, N. Sakai, M. González-Gaitán, S. Matile, A. Roux, *Nat. Chem.* **2018**, *10*, 1118, https://doi.org/10.1038/s41557-018-0127-3.
[5] M. Riggi, K. Niewola-Staszkowska, N. Chiaruttini, A. Colom, B. Kusmider, V. Mercier, S. Soleimanpour, M. Stahl, S. Matile, A. Roux, R. Loewith, *Nat. Cell Biol.* **2018**, *20*, 1043, https://doi.org/10.1038/s41556-018-0150-z.
[6] A. Goujon, A. Colom, K. Straková, V. Mercier, D. Mahecic, S. Manley, N. Sakai, A. Roux, S. Matile, *J. Am. Chem. Soc.* **2019**, *141*, 3380, https://doi.org/10.1021/jacs.8b13189.

[7] V. Mercier, J. Larios, G. Molinard, A. Goujon, S. Matile, J. Gruenberg, A. Roux, *Nat. Cell Biol.* **2020**, *22*, 947, https://doi.org/10.1038/s41556-020-0546-4.

[8] D. Mahecic, L. Carlini, T. Kleele, A. Colom, A. Goujon, S. Matile, A. Roux, S. Manley, *Cell Rep.* **2021**, *35*, 108947, https://doi.org/10.1016/j.celrep.2021.108947.

[9] M. Macchione, M. Tsemperouli, A. Goujon, A. R. Mallia, N. Sakai, K. Sugihara, S. Matile, *Helv. Chim. Acta* **2018**, *101*, e1800014, https://doi.org/10.1002/hlca.201800014.

[10] Q. Verolet, A. Rosspeintner, S. Soleimanpour, N. Sakai, E. Vauthey, S. Matile, *J. Am. Chem. Soc.* **2015**, *137*, 15644, https://doi.org/10.1021/jacs.5b10879.

[11] S. P. H. Mee, V. Lee, J. E. Baldwin, *Chem. Eur. J.* **2005**, *11*, 3294, https://doi.org/10.1002/chem.200401162.

[12] B. Baumeister, S. Matile, *Chem. Eur. J.* **2000**, *6*, 1739, https://doi.org/10.1002/(SICI)1521-3765(20000515)6:10<1739::AID-CHEM1739>3.0.CO;2-Y.

[13] A. P. Gamiz-Hernandez, I. N. Angelova, R. Send, D. Sundholm, V. R. I. Kaila, *Angew. Chem. Int. Ed.* **2015**, *54*, 11564, https://doi.org/10.1002/ange.201501609.

[14] M. Sheves, K. Nakanishi, B. Honig, *J. Am. Chem. Soc.* **1979**, *101*, 7086, https://doi.org/10.1021/ja00517a061.

[15] L. Vogel, P. Wonner, S. M. Huber, *Angew. Chem. Int. Ed.* **2019**, *58*, 1880, https://doi.org/10.1002/anie.201809432.

[16] K. Strakova, L. Assies, A. Goujon, F. Piazzolla, H. V. Humeniuk, S. Matile, *Chem. Rev.* **2019**, *119*, 10977, https://doi.org/10.1021/acs.chemrev.9b00279.

[17] V. Kumar, Y. Xu, D. L. Bryce, *Chem. Eur. J.* **2020**, *26*, 3275, https://doi.org/10.1002/chem.201904795.

[18] P. Scilabra, G. Terraneo, G. Resnati, *Acc. Chem. Res.* **2019**, *52*, 1313, https://doi.org/10.1021/acs.accounts.9b00037.

[19] A. Bauzá, T. J. Mooibroek, A. Frontera, *ChemPhysChem* **2015**, *16*, 2496, https://doi.org/10.1002/cphc.201500314.

[20] B. R. Beno, K.-S. Yeung, M. D. Bartberger, L. D. Pennington, N. A. Meanwell, *J. Med. Chem.* **2015**, *58*, 4383, https://doi.org/10.1021/jm501853m.

[21] K. Strakova, A. I. Poblador-Bahamonde, N. Sakai, S. Matile, *Chem. Eur. J.* **2019**, *25*, 14935, https://doi.org/10.1002/chem.201903604

[22] M. Macchione, N. Chuard, N. Sakai, S. Matile, *ChemPlusChem* **2017**, *82*, 1062, https://doi.org/10.1002/cplu.201600634.

[23] G. Licari, K. Strakova, S. Matile, E. Tajkhorshid, *Chem. Sci.* **2020**, *11*, 5637, https://doi.org/10.1039/D0SC02175J.

[24] M. Páez-Pérez, I. López-Duarte, A. Vysniauskas, N. J. Brooks, M. K. Kuimova, *Chem. Sci.* **2020**, *12*, 2604, https://doi.org/10.1039/D0SC05874B.

[25] F. Piazzolla, V. Mercier, L. Assies, N. Sakai, A. Roux, S. Matile, *Angew. Chem. Int. Ed.* **2021**, *60*, 12258, https://doi.org/10.1002/anie.202016105.

[26] M. Riggi, C. Bourgoint, M. Macchione, S. Matile, R. Loewith, A. Roux, *J. Cell Biol.* **2019**, *218*, 2265, https://doi.org/10.1083/jcb.201901096.

[27] M. Riggi, B. Kusmider, R. Loewith, *J. Cell Sci*. **2020**, *133*, jcs242040, https://doi.org/10.1242/jcs.242040.

[28] N. Jiménez-Rojo, M. D. Leonetti, V. Zoni, A. Colom, S. Feng, N. R. Iyengar, S. Matile, A. Roux, S. Vanni, J. S. Weissman, H. Riezman, *Curr. Biol.* **2020**, *30*, 3775, https://doi.org/10.1016/j.cub.2020.07.059.

[29] C. Roffay, G. Molinard, K. Kim, V. Barbarassa, M. Urbanska, V. Mercier, J. García-Calvo, S. Matile, J. Guck, M. Lenz, A. Roux, *Proc. Natl. Acad. Sci. USA,* **2021,** 118, e2103228118, https://doi.org/10.1073/pnas.2103228118

[30] J. López-Andarias, K. Straková, R. Martinent, N. Jiménez-Rojo, H. Riezman, N. Sakai, S. Matile, *JACS Au* **2021**, *1*, 221, https://doi.org/10.1021/jacsau.0c00069.

[31] J. Hetmanski, H. de Belly, I. Busnelli, T. Waring, R. Nair, V. Sokleva, O. Dobre, A. Cameron, N. Gauthier, C. Lamaze, J. Swift, A. del Campo, T. Starborg, T. Zech, J. Goetz, E. Paluch, J. Schwartz, P. Caswell, *Dev. Cell* **2019**, *51*, 460, https://doi.org/10.1016/j.devcel.2019.09.006.

[32] F. Zuttion, A. Colom, S. Matile, D. Farago, F. Pompeo, J. Kokavecz, A. Galinier, J. Sturgis, I. Casuso, *Nat. Commun*. **2020**, *11*, 536, https://doi.org/10.1038/s41467-020-19710-z.

[33] J. Wang, W. Tan, G. Li, D. Wu, H. He, J. Xu, M. Yi, Y. Zhang, S. A. Aghvami, S. Fraden, B. Xu, *Chem. Eur. J.* **2020**, *26*, 15116, https://doi.org/10.1002/chem.202002974.

[34] S. Wong, S. Lenzini, R. Bargi, Z. Feng, C. Macaraniag, J. Lee, Z. Peng, J. Shin, *Adv. Sci.* **2020**, *7*, 202001066, https://doi.org/10.1002/advs.202001066.

[35] S. Wang, S. Cao, M. Arhatte, D. Li, Y. Shi, S. Kurz, J. Hu, L. Wang, J. Shao, A. Atzberger, Z. Wang, C. Wang, W. Zang, I. Fleming, N. Wettschureck, E. Honore, S. Offermanns, *Nat. Commun.* **2020**, *11*, 2303, https://doi.org/10.1038/s41467-020-16026-w.

[36] T. Sansen, D. Sanchez-Fuentes, R. Rathar, A. Colom-Diego, F. El Alaoui, J. Viaud, M. Macchione, S. de Rossi, S. Matile, R. Gaudin, V. Backer, A. Carretero-Genevrier, L. Picas, *ACS Appl. Mater. Interfaces* **2020**, *12*, 29000, https://doi.org/10.1021/acsami.0c05432.

[37] K. Rahman, C. Coomer, S. Majdoul, S. Ding, S. Padilla-Parra, A. Compton, *eLife* **2020**, *9*, e58537, https://doi.org/10.7554/eLife.58537.

[38] L. Oberhauser, S. Granziera, A. Colom, A. Goujon, V. Lavallard, S. Matile, A. Roux, T. Brun, P. Maechler, *Biochim. Biophys. Acta, Mol. Cell Res.* **2020**, *1867*, 118619, https://doi.org/10.1016/j.bbamcr.2019.118619.

[39] M. Nava, Y. Miroshnikova, L. Biggs, D. Whitefield, F. Metge, J. Boucas, H. Vihinen, E. Jokitalo, X. Li, J. Arcos, B. Hoffmann, R. Merkel, C. Niessen, K. Dahl, S. Wickstrom, *Cell* **2020**, *181*, 800, https://doi.org/10.1016/j.cell.2020.03.052.

[40] S. Gupta, J. Yano, V. Mercier, H. H. Htwe, H. R. Shin, G. Rademaker, Z. Cakir, T. Ituarte, K. W. Wen, G. E. Kim, R. Zoncu, A. Roux, D. W. Dawson, R. M. Perera, *Nat. Cell Biol.* **2021**, *23*, 232, https://doi.org/10.1038/s41556-021-00644-7.

[41] C. A. Coomer, I. Carlon-Andres, M. Iliopoulou, M. L. Dustin, E. B. Compeer, A. A. Compton, S. Padilla-Parra, *PLoS Pathog.* **2020**, *16*, e1008359, https://doi.org/10.1371/journal.ppat.1008359.

[42] A. F. L. Schneider, M. Kithil, M. C. Cardoso, M. Lehmann, C. P. R. Hackenberger, *Nat. Chem.* **2021**, *13*, 530, https://doi.org/10.1038/s41557-021-00661-x.

[43] F. Neuhaus, F. Zobi, G. Brezesinski, M. Dal Molin, S. Matile, A. Zumbuehl, *Beilstein J. Org. Chem.* **2017**, *13*, 1099, https://doi.org/10.3762/bjoc.13.109.

[44] G. Licari, J. S. Beckwith, S. Soleimanpour, S. Matile, E. Vauthey, *Phys. Chem. Chem. Phys*. **2018**, *20*, 9328, https://doi.org/10.1039/C8CP00773J.

[45] M. Tsemperouli, E. Amstad, N. Sakai, S. Matile, K. Sugihara, *Langmuir* **2019**, *35*, 8748, https://doi.org/10.1021/acs.langmuir.9b00673.

[46] D. I. Danylchuk, P.-H. Jouard, A. S. Klymchenko, *J. Am. Chem. Soc*. **2021**, *143*, 912, https://doi.org/10.1021/jacs.0c10972.

[47] N. Li, W. Zhang, H. Lin, J.-M. Lin, *Chin. Chem. Lett*. **2021**, in press, https://doi.org/10.1016/j.cclet.2021.08.060.

[48] J. García-Calvo, J. López-Andarias, J. Maillard, V. Mercier, C. Roffay, A. Roux, A. Fürstenberg, N. Sakai, S. Matile, in preparation, **2021**.

[49] M. Macchione, A. Goujon, K. Strakova, H. V. Humeniuk, G. Licari, E. Tajkhorshid, N. Sakai, S. Matile, *Angew. Chem. Int. Ed.* **2019**, *58*, 15752, https://doi.org/10.1002/anie.201909741.

[50] J. E. Chambers, M. Kubánková, R. G. Huber, I. López-Duarte, E. Avezov, P. J. Bond, S. J. Marciniak, M. K. Kuimova, *ACS Nano* **2018**, *12*, 4398, https://doi.org/10.1021/acsnano.8b00177.

[51] L. Yu, J. F. Zhang, M. Li, D. Jiang, Y. Zhou, P. Verwilst, J. S. Kim, *Chem. Commun.* **2020**, *56*, 6684, https://doi.org/10.1039/D0CC02943B.

[52] Z. Zhang, G. Sun, W. Chen, J. Su, H. Tian, *Chem. Sci.* **2020**, *11*, 7525, https://doi.org/10.1039/D0SC01591A.

[53] R. Kimura, H. Kuramochi, P. Liu, T. Yamakado, A. Osuka, T. Tahara, S. Saito, *Angew. Chem. Int. Ed*. **2020**, *59*, 16430, https://doi.org/10.1002/anie.202006198.

[54] A. S. Klymchenko, A. P. Demchenko, *J. Am. Chem. Soc.* **2002**, *124*, 12372, https://doi.org/10.1021/ja027669l.

[55] N. Sakai, S. Matile, *J. Am. Chem. Soc*. **2018**, *140*, 11438, https://doi.org/10.1021/jacs.8b06668.

[56] K. Straková, J. López-Andarias, N. Jiménez-Rojo, J. E. Chambers, S. J. Marciniak, H. Riezman, N. Sakai, S. Matile, *ACS Cent. Sci*. **2020**, *6*, 1376, https://doi.org/10.1021/acscentsci.0c00666.

[57] J. López-Andarias, K. Ebligatian, Q. T. L. Pasquer, L. Assies, N. Sakai, S. Hoogendoorn, S. Matile, *Angew. Chem. Int. Ed.* in press, https://doi.org/10.1002/anie.202113163.

[58] J. García-Calvo, J. Maillard, I. Fureraj, K. Strakova, A. Colom, V. Mercier, A. Roux, E. Vauthey, N. Sakai, A. Fürstenberg, S. Matile, *J. Am. Chem. Soc.* **2020**, *142*, 12034, https://doi.org/10.1021/jacs.0c04942.